Vol. No.6, Issue No. 08, August 2017 www.ijarse.com



Curvelet Transform and Adaboost Technique for HSI Feature Extraction

Y.Vasudeva rao¹, T.Geetamma²,

¹ECE Department, M.Tech Scholar, DECS, GMRIT, (India) ²ECE Departments, AssistantProfessor, GMRIT, (India)

ABSTRACT

Generally, Spectral component extraction methods are connected to the HSI information shape straightforwardly. This paper shows a novel calculation for HSI include extraction by abusing the curvelet transformed space by means of a moderately new unearthly component preparing procedure—solitary range examination (SSA). Utilizing the support vector machine classifier, trial comes about have demonstrated that elements separated by SSA on curvelet coefficients have better execution regarding grouping precision over components removed on wavelet coefficients. Since the proposed approach primarily depends on SSA for include extraction on the ghostly measurement, it really has a place with the ghastly element extraction classification. Subsequently, the proposed strategy has likewise been contrasted and some cutting edge otherworldly element extraction procedures to demonstrate its viability. Furthermore, adaboost technique is used for classification and denoising of images. By which we can obtain good feature extraction of images.

Keywords: HSI, SVM, Curvelet Transform, Single Spectrum Analysis

I. INTRODUCTION

Hyperspectral imaging (HSI) provides data with ahigh-resolution spectrum over 2-D images, leading topowerful capabilities related to classification in many applications, such as remote sensing. The wide range covered by thespectral information, from visible light to near infrared, allowsthe recognition of small differential characteristics of the contentin a scene. For that reason, new emerging laboratory-baseddata analysis, including food quality, medical, or verification of counterfeit goods and documents [1]–[4], is based on HSI. The use of the support vector machine (SVM) as a classifierfor HSI applications has been shown to be robust and highlyaccurate [5]–[7]. The samples or pixels are evaluated in SVMby means of their respective features or spectral bands, whichcan contribute to more robust discrimination as they include information from different spectral wavelengths. However, HSIdata are usually prone to noise, which can reduce the discriminationability limiting the accuracy in classification tasks. Forthat reason, there is great interest for a potential decomposition of the spectral profiles into components in such a way that noisecould be removed or mitigated by avoiding particular components with high noisy content. In this decomposition context, a particularly interesting research area is the use of the empirical mode decomposition (EMD) technique applied in 1-Dto the spectral profile of the pixels as briefly evaluated in [8]. The EMD is the main part of the Hilbert–Huang transform, an algorithm for the analysis of nonlinear and nonstationarytime series [9], [10]. EMD

Vol. No.6, Issue No. 08, August 2017

www.ijarse.com



decomposes a 1-D signal into afew components called intrinsic mode functions (IMFs) andhas been widely used in processing signal applications such asspeech recognition [11]. Hence, our aim is to introduce the singular spectrum analysis(SSA) technique in a similar way to evaluate its performance for classification tasks in HSI. In this paper, we are also aiming at combining ideas offeature extraction and denoising together for improving classification accuracy of remote sensing hyperspectral images. Finally, Adaboost technique is applied inorder to increase the rate of accuracy.

II. CURVELET TRANSFORM:

For multi-scale object representation, Curvelets are a non-adaptive technique. Being an extension of the wavelet concept, they are becoming popular in similar fields ofscientific computing and image processing. By using a basis that represents both location and spatial frequency, wavelets generalize Fourier transform. Directional wavelet transforms go further for 2D or 3D signals, by using basis functions that are also localized in orientation. From other directional wavelet transforms, a curvelet transform differs as such the degree of localization in orientation varies with scale. In particular, fine-scale basis functions are long ridges; the shape of the basis functions at scale j is 2^{-j} by $2^{-j/2}$ so the fine-scale bases are skinny ridges with a

precisely determined orientation.

For representing images (or other functions) which are smooth apart from singularities along smooth curves, where the curves have bounded curvature, the curvelets are an appropriate basis. i.e. for images where objects in it have a minimum length scale. For cartoons, geometrical diagrams, and text this property holds. The edges such images contain appear increasingly straightwhen one zooms in on them. By defining higher resolution curvelets to be more elongated than the lower resolution ones, Curvelets take advantage of this property. However, natural images (photographs) do not have this property; they have detail at every scale. Therefore, it is preferable to use some sort of directional wavelet transformfor natural images, whose wavelets have the same aspect ratio at every scale.

When the image is of the right type, curvelets provide a representation that is considerably sparser than other wavelet transforms. This can be quantified by considering the best approximation of a geometrical test image that can be represented using only 'n' wavelets, and analysing the approximation error as a function of 'n'. The squared error decreases only as $O(\frac{1}{\sqrt{n}})$ for a Fourier transform. For a wide variety of wavelet transforms,

including both directional and non-directional variants, the squared error decreases as $O(\frac{1}{n})$. The extra assumption underlying the curvelet transform allows it to achieve $O((\log n)^2/n^2)$..

For computing the curvelet transform of discrete data, efficient numerical algorithms exist. The computational cost of a curvelet transform is approximately 10-20 times that of an FFT, and has the same dependence of $O(n^2 \log n)n^2 \log n$ for an image of size $nn \times n$.

Vol. No.6, Issue No. 08, August 2017 www.ijarse.com



2.1. From Classical Wavelet to curvelet Transform:

Although the DWTs has established an impressive reputation as a tool for mathematical analysis and signal processing, it has the disadvantage of poor directionality, which has undermined its usage in many applications. transformIn recent years significant progress in development of directional wavelets has been made. To improve directional selectivity, complex wavelet is one way. However, the complex wavelet transform has not been widely used in the past, since it is difficult to design complex wavelets with perfect reconstruction properties and good filter characteristics.By essentially using tensor-product one-dimensional (1-D) wavelets,the 2-D complex wavelets are constructed. The directional selectivity provided by complex wavelets (six directions) is much better than that obtained by the classical DWTs (three directions), but is still limited.

In 1999, Candès and Donoho proposed an anisotropic geometric wavelet transform named ridgelet transform which is optimal at representing straight-line singularities. Unfortunately, global straight-line singularities are rarely observed in real applications. To analyze local line or curve singularities, a natural idea is to consider a partition of the image, and then to apply the ridgelet transform to the obtained subimages. This block ridgeletbased transform, which is named curvelet transform, was first proposed by Candès and Donoho in 2000. Apart from the blocking effects, however, the application of this so-called first-generation curvelet transform is limited because the geometry of ridgelets is itself unclear, as they are not true ridge functions in digital images. Later, a considerably simpler second-generation curvelet transform based on a frequency partition technique was proposed by same authors. A variant of the second-generation curvelet transform was proposed recently, to handle image boundaries by mirror extension (ME). Previous versions of the transform treated image boundaries by periodization. Here, the main modifications are to tile the discrete cosine domain instead of discrete Fourier domain and to adequately reorganize data. The computational complexity of the obtained algorithm and the standard curvelet transform are same. The second-generation curvelet transform has been shown to be a very efficient tool for many different applications in solving partial different equations (PDEs), image processing, seismic data exploration and fluid mechanics. In this survey, we will focus on this successful approach and show its numerical and theoretical aspects as well as the different applications of curvelets.

The strength of the curvelet approach is their ability to formulate strong theorems in approximation and operator theory, from the mathematical point of view. To represent curve-like edgesthe discrete curvelet transform is very efficient. However, the current curvelet systems still have two main drawbacks: 1) they are not optimal for sparse approximation of curve features beyond C2-singularities, and 2) the discrete curvelet transform is highly redundant. The currently available implementations of the discrete curvelet transform (see www.curvelet.org) aim to reduce the redundancy smartly. However, independently from the good theoretical results on N-term approximation by curvelets, the discrete curvelet transform is not appropriate for image compression. The question of how to construct an orthogonal curvelet-like transform is still open. There have been several other developments of directional wavelet systems in recent years with the same goal, namely a better analysis and an optimal representation of directional features of signals in higher dimensions. None of these approaches has reached the same publicity as the curvelet transform. However, we want to mention shortly some of these developments and also describe their relationship to curvelets.

Vol. No.6, Issue No. 08, August 2017 www.ijarse.com



This feature is paid by high redundancy. Applications of Gabor wavelets focused on image classification and texture analysis. Gabor wavelets have also been used for modeling the receptive field profiles of cortical simple cells. Applications of Gabor wavelets suggested that the precision in resolution achieved through redundancy may be a relevant issue in brain modeling, and that orientation plays a key role in the primary visual cortex. The main differences between steerable wavelets/ Gabor wavelets and other X-lets is that the early methods do not allow for a different number of directions at each scale.

Contourlets, as proposed by Do and Vetterli, form a discrete filter bank structure that can deal effectively with piecewise smooth images with smooth contours. This discrete transform can be connected to curvelet-like structures in the continuous domain. Hence, the contourlet transform can be seen as a discrete form of a particular curvelet transform. Curvelet constructions require a rotation operation and correspond to a partition of the 2-D frequency plane based on polar coordinates; see the section "The Discrete Curvelet Frame." This property is what makes the curvelet idea simple in the continuous case but causes problems in the implementation for discrete images. In particular, approaching critical sampling seems difficult in discretized constructions of curvelets. Critically sampling is easy to implement for contourlets. The directional filter bank, as a key component of contourlets, has a convenient tree-structure, where aliasing is allowed to exist and will be cancelled by carefully designed filters. The 3-D extensions of the 2-D contourlets are Surfacelets, that are obtained by a higher-dimensional directional filter bank and a multiscale pyramid. They can be used to efficiently capture and represent surface-like singularities in multidimensional volumetric data involving biomedical imaging, seismic imaging, video processing and computer vision. Surfacelets and the 3-D curvelets (see the section "Three-Dimensional Curvelet Transform") aim at the same frequency partitioning, However, these two transforms achieve this goal with different approaches as we described above in the 2-D case.

III. SINGULAR SPECTRAL ANALYSIS(SSA):

The singular spectrum analysis(SSA) is a nonparametric spectral estimation method in time series analysis. Itcombines the elements of classical time series analysis, multivariate statistics, multivariate geometry, dynamical systems and signal processing. SSA is a nonparametric method. It tries to overcome the problems of finite sample length and noisiness of sampled time series not by fitting an assumed model to the available series, but by using a data-adaptive basis set, instead of the fixed sine and cosine of the Blackman-Tukey method.

There are three basic steps in SSA: i) embedding the sampled time series in a vector space of dimension M; ii) computing the MxM lag-covariance matrix C_D of the data; and iii) diagonalizing C_D .

Step (i): The time series $\{x(t): t=1,N\}$ is embedded into a vector space of dimension M by considering M laggedcopies $\{x(t-j): j=1,....M\}$ thereof. The choice of the dimension M is not obvious, but SSA is typically successful at analyzing periods in the range (M/5, M).

Step (ii): One defines the MxM lag-covariance matrix estimator C_D . There are three distinct methods used widely to define C_D . In the BK (Broomhead and King) algorithm, a window of length M is moved along the time series, producing a sequence of N'=N-M+1 vectors in the embedding space. This sequence is used to obtain the N' x M trajectory matrix D, where the i-th row is the i-th view of the time series through the window. In this approach, C_D is defined by:

Vol. No.6, Issue No. 08, August 2017 www.ijarse.com



$$C_D = \frac{1}{N'} D^T D$$

In the VG algorithm, C_D is estimated directly from the data as a Toeplitz matrix with constant diagonals, i.e., its entries C_{ij} depend only on the lag |i-j|:

$$c_{ij} = \frac{1}{N - |i - j|} \sum_{t=1}^{N - |i - j|} x(t)x(t + |i - j|)$$

Burg covariance estimation is an iterative process based on fitting an AR model with a number- of AR components equal to the SSA window length. Both the Burg and VG methods impose a Toeplitz structure upon the autocovariance matrix whereas the BK method does not. The Burg approach in principal should involve less "power leakage" due to the finite length of the time series and should therefore improve resolution. However, the Burg estimate can induce significant biases when nonstationarities and very low-frequency variations are present in the series. Thus in some cases to try the VG method will worth a while. Also, for long series (N on the order of 5,000), the VG estimate is less computationally burdensome and thus is completed more quickly. In practice, the VG method is more prone than is the Burg method to numerical instabilities (yielding negative eigenvalues) when pure oscillations are analyzed. The BK method is thus somewhat less prone to problems with nonstationary time series, although the VG method seems untroubled by all but the most extreme nonstationarities. However the Toeplitz methods do appear to yield more stable results under the influence of Step (iii): The covariance matrix calculated from the N sample points, is then diagonalized and the eigenvalues are ranked in decreasing order. The eigenvalue {&lambda_k, k=1,...,M} gives the variance of the time series in the direction specified by the corresponding eigenvector E_k , the square roots of the eigenvalues are called singular values and the corresponding set the singular spectrum. These terms give SSA its name; BK showed how to obtain singular spectrum by SVD applied to the trajectory matrix D. VG called the E_k's temporal empirical orthogonal functions (EOFs), by analogy with the meteorological term used when applying PCA in the spatial domain.

3.1. Principal of SSA:

SSA is a recent technique of time-series analysis and forecasting with multiple potential in different applications, going from market research or social science to data mining. Withorigin in the former Soviet Union during the 1980s, there are several related publications in the last 20 years, although some authors stand out [12], [13]. Here, the SSA concept and capabilities are briefly introduced, along with a complete mathematical description of the algorithm and a practical example for an easy understanding.

Vol. No.6, Issue No. 08, August 2017 www.ijarse.com



3.2.Concept

To decompose an original series into several independent components or subseries is the main objective of SSA. These components are interpretable, i.e., they can be mainly identified as varying trend, oscillations, or noise. Therefore, the main capabilities of SSA can be summarized as follows [12]:

- 1) extraction of trends, periodic components, and smoothing;
- 2) complex trends and periodicities with varyingamplitudes;
- 3) finding structures in short time series;
- 4) envelopes of oscillating signals.

All these capabilities make SSA a really interesting approach, particularly as most research studies have not yet takenit into consideration in HSI.

3.4.Application of SSA

Given a particular sample, e.g., a spectral pixel in HSI,the SSA aims to achieve improved reconstruction of the pixelprofile by means of the main eigenvalue components whileabandoning the less representative or noisy components. Foreffective reconstruction of the original profile, there are twoimportant parameters affecting the performance. The window size L is the first parameter, which determines the total number of components that can be extracted in the decomposition stage. Taking L=10, for example, ten eigenvalues are extracted, which leads to ten potential components generated. Obviously, the component corresponding to the first eigenvalue is much more significant than those corresponding to the following eigenvalues. The second parameter, i.e., eigenvalue grouping (EVG), denotes the selected combination of extracted components used for reconstruction. Theuse of only the first two components will remove most noise from the input data, for a data set with highly noisy content. However, if the noise level is low that only affects small components such as the ninth or the tenth, using just the first two components in the reconstructed signal maylead to loss of discriminating information in the samples.

IV. PROPOSED METHODOLOGY

The proposed denoising andfeature extraction approach will be applied on hyperspectralimages, and the flowchart is shown in Fig. 1 for reference. Hyperspectral sensors have a relatively high spectral resolution and can generate hundreds of observation channels. The obtained 3-D HSI data cube can be regarded as a stack of 2-D images of the same scene corresponding to different wavelengths, and the correlation between each two adjacent bands is fairly high.

Vol. No.6, Issue No. 08, August 2017 www.ijarse.com



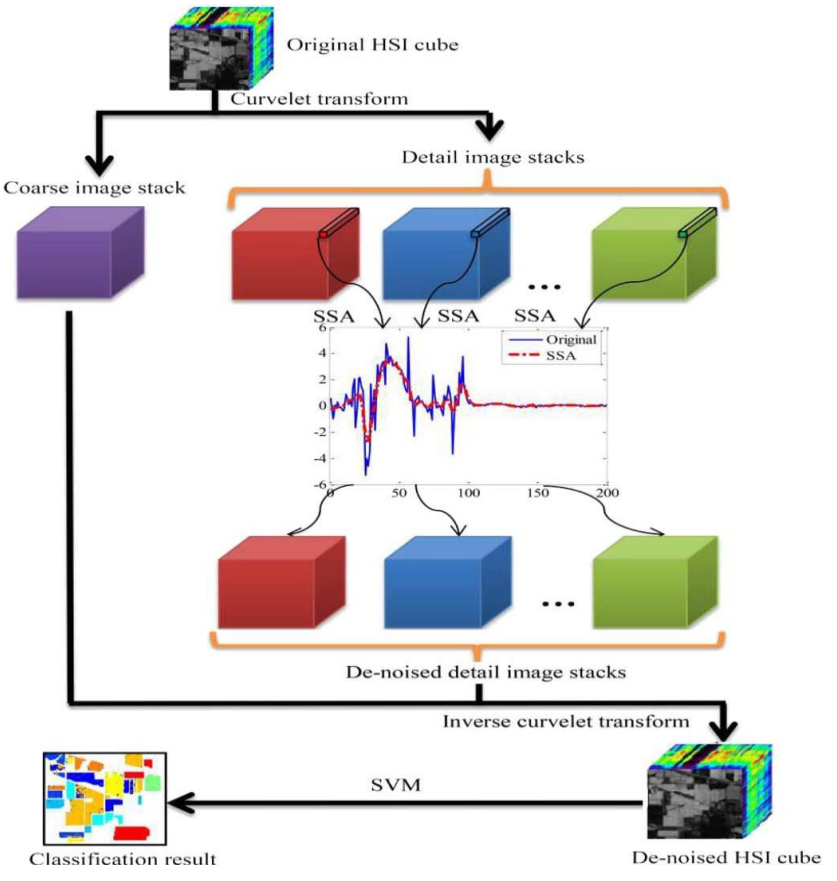


Fig 1. Proposed Methodology

In the proposed method, the first step of theis to perform the curvelet transform on each band of thehyperspectral image, and a few image stacks are generated after the transform as shown in Fig. 1. By applying the curvelettransform on each band, the band correlation property can be preserved so that SSA is able to exploit the spectral signature. To apply SSA in the spectral dimension for each detail image stack for feature extraction and denoising is the next step. After that, the denoised detail images at each band are gathered according to their original location, followed by the inverse curvelet transform to get the denoised hyperspectral image.

4. 1 Applying SSAIn The Curvelet Domain

In this paper, a hyperspectral image is denoted as $I(p, q) = (I1(p, q), I2(p, q), \dots, IB(p, q)) \in B$, where $p \in [1,P], q \in [1,Q], P \times Q$ is the spatial dimension of the hyperspectralimage, and B is the number of bands. represents the setof real numbers with the pixel intensity Ib(p, q) at all sensorchannels with $b \in [1,B]$. The 2-D curvelet transform viaUSFFT employed in this paper is completed using the toolboxCurveLab (version 2.1.2) [38]. Similar to the wavelet transform,the curvelet transform can also decompose the imageinto a coarse image and several detail images. Just like mostimage processing algorithms, the curvelet transform requiresthe processed image to be a square whose dimension is a power of 2. If the size of the original image is not a power of 2, pixelswith a value of zero are padded to the next larger power of 2. Given the zero-padded HSI data set, $I_pad(m, n) = (I_pad1(m, n), I_pad2(m, n), \dots, I_padB(m, n))$ where $m, n \in [1,N]$, consisting of B bands where

Vol. No.6, Issue No. 08, August 2017

www.ijarse.com



each band has N2 pixels, the curvelet transform is performed on a band image I_padb to obtain the curvelet coefficients corresponding to that band e_b^D , i.e.,

$$c_b^D = CT(I_{pad_b})$$

where CT stands for the discrete curvelet transform operation explained in Section II. The decomposition results of the transformcan be regarded as a superposition in the following form:

$$c_b^D = c_{b,j} + \sum_{j=1}^{j-1} W_{b,j}$$

where $c_{b,j}$ is the coarse version of the original band image withlow-frequency contents, and $W_{b,j}$ stands for the detail bandimage at scale 2-j containing high-frequency contents. With anN \times N image, the default number of decomposition scales is J = log 2(N) - 3 as set in the CurveLab toolbox. Take a bandimage with the size of 128 \times 128 for instance, the number ofdecomposition scales J will be four. According to the settingsin the toolbox, there are eight orientations of the curvelet in thesecond and third scales, starting from the top-left wedge and an according in a clockwise fashion, but for the coarsest and finestscales, there is only one direction. Thus,

$$C_b^D = C_{b,l,1} + W_{b,1,1} + \sum_{j=2}^{J-1} \sum_{l=1}^g W_{b,j,l}$$

where $W_{b,1,1}$ represents the finest scale with one orientation. The schematic of four decomposition scales corresponding to a 128×128 image is shown in Fig. 2. Then, after applying the curvelet transform to all bands, there will be a coarse imagestack and 17 detail image stacks.

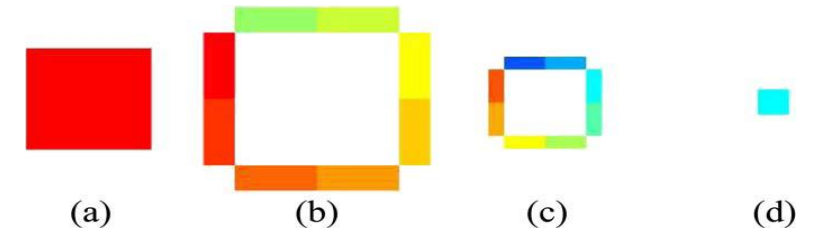


Fig. 2. Illustration of a 128×128 image with four decomposition scales.(a) First (finest) scale with one orientation. (b) Second scale with eightorientations. (c) Third scale with eight orientations. (d) Fourth (coarsest) scalewith one orientation.

V. RESULTS

Fig 3 shows the Indian Pines data set which was collected in the Indian Pines test site in Northwest Indiana, USA on June 12, 1992. The scene consists of two-thirds agriculture, and one-third forest, or other natural perennial vegetation

Vol. No.6, Issue No. 08, August 2017 www.ijarse.com





Fig 3. Input Image

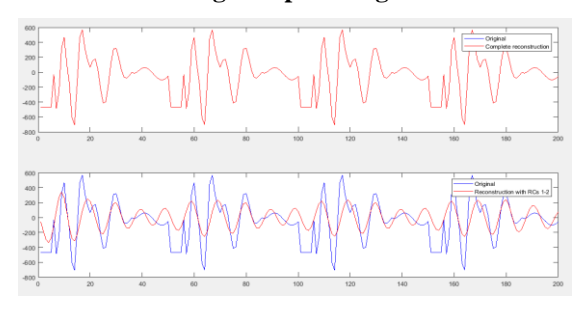


Fig 4. Reconstruction image

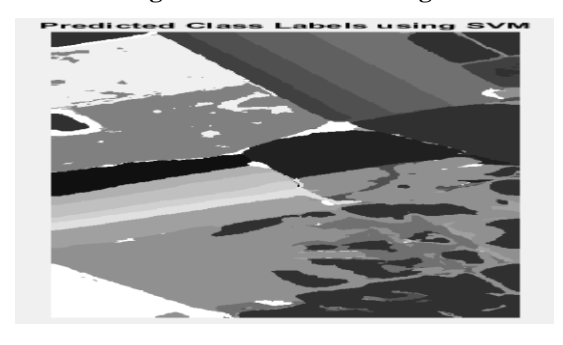


Fig 5. SVM Classified image

The above fig 5 shows the classification results of Indian pine data for the given original data. It is obtained by doing SVM classification.

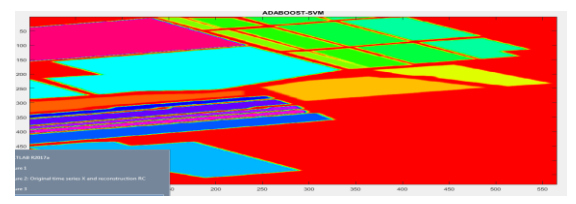


Fig 6. Adaboost SVM output

fig 6 shows adaboost svm output that avoids errors and get a more consistent result and obtain more accuracy.

mean class-by-class and average and overall accuracy values (%) of ten repeated experiments on testing samples of the original indian pine data set and ssa, ct-ssa, adaboost-ct-, followed by the standard deviation

Vol. No.6, Issue No. 08, August 2017 www.ijarse.com



Accuracy: SSA CT-SSA ADABOOST-CTSSA	
Class 1: 87.038500 90.460000 90.730000	
Class 2:88.918500 92.340000 92.610000	
Class 3: 91.098500 94.520000 94.790000	
Class 4:90.328500 93.750000 94.020000	
Class 5 : 90.728500 94.150000 94.420000	
Class 6: 95.768500 99.190000 99.460000	
Class 7: 91.508500 94.930000 95.200000	
Class 8: 95.898500 99.320000 99.590000	
Class 9: 88.838500 92.260000 92.530000	
Class 10: 88.418500 91.840000 92.110000	
Class 11: 90.898500 94.320000 94.590000	
Class 12: 88.388500 91.810000 92.080000	
Class 13: 93.108500 96.53000096.800000	
Class 14: 96.268500 99.690000 99.960000	
OA : 91.708500 95.130000 95.400000	
AA : 92.438500	

Accuracy: (predicted class label) / (actual class label)

Since the proposed methodology is inspired by the feature extraction approach based on SSA. the proposed approach is denoted as CT-SSA, and other inspirational approaches are named SSA. The proposed CT-SSA approach actually belongs to the 1-Dspectral processing technique for hyperspectralimages. The testing is performed on different classes and the accuracy is been calculated. The accuracy is compared between SSA, CT-SSA and Adaboost-CT-SSA. Adaboost-CT-SSA is obtained good state of accuracy compared to SSA and CT SSA. When compared with only SSA, CT-SSA has better performance. It can be seen that those dimensionality reduction techniques only give comparable results compared with the original dataset, although they could speed up the classification process. Highest classification OA and AA achieved by Adaboost-CT-SSA.

VI. CONCLUSION

In this paper, two powerful tools, i.e., SSA and the curvelet transform, are combined for HSI feature extraction. By applying SSA in the curvelet domain, noise can be smoothed from the decomposed signals, resulting in more effective feature extraction. Inspired by applying PCA in the curvelet domain and another method of solely applying SSA on HSI data, the proposed method adaboost technology takes advantage of those approaches. By

Vol. No.6, Issue No. 08, August 2017

www.ijarse.com



using this adaboost technology the feature extraction made more accurate and the noise smoothen is high compared to other techniques.

REFERENCES

- [1] V. E. Brando and A. G. Dekker, "Satellite hyperspectral remote sensing for estimating estuarine and coastal water quality," IEEE Trans. Geosci.Remote Sens., vol. 41, no. 6, pp. 1378–1387, Jun. 2003.
- [2] J. Ren, S. Marshall, C. Craigie, and C. Maltin, "Quantitative assessment of beef quality with hyperspectral imaging using machine learning techniques," in Proc. 3rd Int. Conf. Hyperspectral Imaging, 2012, pp. 72–75.
- [3] K. Gill, J. Ren, S. Marshall, S. Karthick, and J. Gilchrist, "Qualityassuredfingerprint image enhancement and extraction using hyperspectralimaging," in Proc. 4th Int. Conf. Imaging Crime Detect. Prevention, 2011,pp. 1–6.
- [4] T. Nagaoka, A. Nakamura, Y. Kiyohara, and T. Sota, "Melanoma screeningsystem using hyperspectral imager attached to imaging fiberscope," inProc. IEEE Eng. Med. Biol. Soc., 2012, pp. 3728–3731.
- [5] F.Melgani and L. Bruzzone, "Classification of hyperspectral remote sensingimages with support vector machines," IEEE Trans. Geosci. RemoteSens., vol. 42, no. 8, pp. 1778–1790, Aug. 2004.
- [6] M. Pal and G. M. Foody, "Feature selection for classification of hyperspectral by SVM," IEEE Trans. Geosci. Remote Sens., vol. 48, no. 5,pp. 2297–2307, May 2010.
- [7] R. Archibald and G. Fann, "Feature selection and classification of hyperspectralimages with support vector machines," IEEE Geosci. RemoteSens. Lett., vol. 4, no. 4, pp. 674–677, Oct. 2007.
- [8] B. Demir and S. Ertürk, "Empirical mode decomposition of hyperspectralimages for support vector machine classification," IEEE Trans. Geosci.Remote Sens., vol. 48, no. 11, pp. 4071–4084, Nov. 2010.
- [9] N. E. Huang, Z. Shen, S. Long, R. Wu, C. Shih, H. Zheng, Q. Yen, N.-C. Tung, and C. Liu, "The empirical mode decomposition and the Hilbert spectrum for nonlinear and non-stationary time series analysis," Proc. R. Soc. Lond. A, Math. Phys. Sci., vol. 454, no. 1971, pp. 903–995, Mar. 1998.
- [10] G. Rilling, P. Flandrin, and P. Gonçalvés, "On empirical mode decomposition and its algorithms," in Proc. IEEE-EURASIP Workshop NSIP, 2003,vol. 3, pp. 8–11.
- [11] H. Huang and J. Pan, "Speech pitch determination based on Hilbert–Huang transform," Signal Process., vol. 86, no. 4, pp. 792–803, Apr. 2006.
- [12] N. Golyandina and A. Zhigljavsky, Singular Spectrum Analysis for TimeSeries. Berlin, Germany: Springer-Verlag, 2013.
- [13] N. Golyandina, V. Nekrutkin, and A. A. Zhigljavsky, Analysis of TimeSeries Structure: SSA and Related Techniques. London, U.K.: Chapman& Hall, 2001.
- [14] Pursue's University Multispec Site: AVIRIS image Indian Pine Test Site, Jun. 12, 1992. [Online]. Available: https://engineering.purdue.edu/~biehl/MultiSpec/hyperspectral.html
- [15] Hyperspectral Remote Sensing Scenes. [Online]. Available: http://www.ehu.es/ccwintco/index.php/Hyperspectral_Remote_Sensing_Scenes

Vol. No.6, Issue No. 08, August 2017 www.ijarse.com



- [16] A. Linderhed, Image Empirical Mode Decomposition MATLAB Code.[Online]. Available: http://aquador.vovve.net/IEMD/
- [17] J. Zabalza, J. Ren, C. Clemente, G. Di Caterina, and J. J. Soraghan, "Embedded SVM on TMS320C6713 for signal prediction in classificationand regression applications," in Proc. 5th Eur. DSP Educ. Res. Conf., Amsterdam, The Netherlands, Sep. 2012, pp. 90–94.
- [18] C-C. Chang and C-J. Lin, "LIBSVM: A library for support vector machines," ACM Trans. Intell. Syst. Technol., vol. 2, no. 3, pp. 27:1–27:27, Apr. 2011.